Available online at www.sciencedirect.com
SCIENCE DIRECT®
Engineering Failure Analysis 13 (2006) 9–17
ENGINEERING FAILURE ANALYSIS
www.elsevier.com/locate/engfailanal

Failure analysis of turbine disc of an aero engine

Lucjan Witek *

Faculty of Mechanical Engineering and Aeronautics, Rzeszow University of Technology, 8 Powstańców Warszawy Avenue, 35-959 Rzeszów, Poland

Received 23 December 2004; accepted 24 December 2004
Available online 31 March 2005

Abstract

This paper presents the failure analysis of the turbine disc of an aero engine, installed in a certain type of aircraft. From the visual examination of the fractured surface, it was possible to observe beach marks, typical of fatigue failure. A non-linear finite element method was utilized to determine the stress state of the disc/blade segment under operating conditions. High stress zones were found at the region of the lower fir-tree slot, where the failure occurred. A computation were also performed with excessive rotational speed. Attention of this study is devoted to the mechanisms of damage of the turbine disc and also the critical high stress areas.

Keywords: Turbine disc; Failure analysis; Fatigue; Turbine engine; FEM

1. Introduction

The major function of the turbine is to extract energy from the hot gas flow to drive the compressor and the accessory gearbox. Gas turbine discs work mostly at high temperature gradients and are subjected to high rotational velocity. High speed results in large centrifugal forces in discs and simultaneous high temperature reduces disc material strength.

The service life of critical aerospace components is governed by the modes of degradation and failure such as: fatigue, fracture, yielding, creep, corrosion, erosion, wear, etc. Gas turbine discs are usually the most critical engine components, which must endure substantial mechanical and thermal loading. If a problem arises in the turbine section it will significantly affect the whole engine function and, of course, safety of the aircraft. Blade loss can be contained within the engine casing, while the catastrophic failure of a turbine

* Tel.: +48 17 865 1324; fax: +48 69 196 2047.
E-mail address: lwitek@prz.rzeszow.pl.

1350-6307/$ - see front matter
doi:10.1016/j.engfailanal.2004.12.028

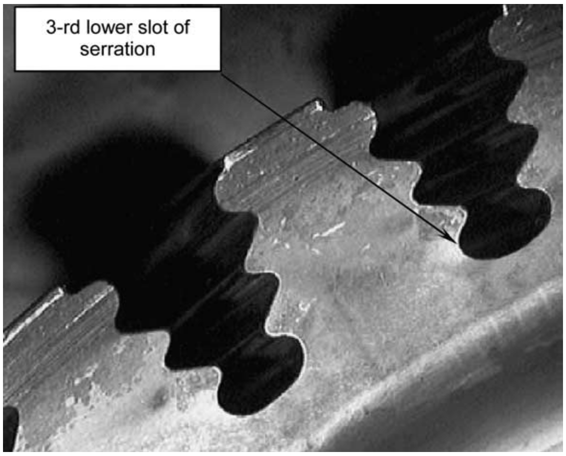

Fig. 1. The dovetail-rim area (fir-tree slots, serration fitting) of turbine disc.

wheel could cause puncture of the engine casing by the larger fragments of the disc. This kind of failure is often concerned with overspeeding of the disc. Excessive rotational speed of turbine is sometimes permissible for aircraft in the case of heavy operational conditions (i.e., short take of from landing ground).

Aeroengine turbine discs basically have three critical regions on which attention should be focused: the dovetail-rim area (fir-tree slots, serration fitting) (Fig. 1), the assembly holes and the hub zone.

The joint between the turbine blade and the disc usually represents the most critical area from the point of view of the static and fatigue approaches. The loads associated with these regions are mainly the centrifugal forces and thermal stresses.

The stress and failure analysis of the jet engine turbine has received the attention of several investigations. The problem of numerical evaluation of stress state in the dovetail-rim area of disc and blade is described by Chan et al. [1], Masataka [2], Meguid et al. [3], Papanikos et al. [4] and Zboinski [5]. Of interest is also work by McEvily [6], in which the author analyzed the failures of engines, used to power the MD-88, DC-10 and B-737 planes. In these cases, the problem of unexpected fatigue failure of the turbine was the reason for the crash of the aircraft. Hou [7] described the experimental and numerical investigation of the phenomena occurring in the fatigue fracture of turbine blades. Using nonlinear FE analysis, the authors specified the phases of the fatigue process. The problem of fatigue fracture of turbine components was also described by Bhaumik [8] and Park et al. [9]. The consequences of such failure are particularly dangerous, resulting in the destruction of the engine and ultimately in loss of life.

In this study, attention is devoted to analysis of the damage mechanisms of the turbine disc subjected to both operational and overspeed conditions and also to indicate critical areas, from the point of view of the stress analysis. The additional goal of this analysis is to improve the safety and reliability of the aircraft and different planes, powered by the same type of engine.

2. Visual examination of failed disc

The fractured disc was first subjected to visual examination. The disc failure location is presented in Fig. 2. As seen from this figure, the disc first fractured in the zone of the lower fir-tree slot of the serrations. After that, small fractured pieces of disc in common with the three separated blades damaged the other blades. These damaged blades are visible in Fig. 2.

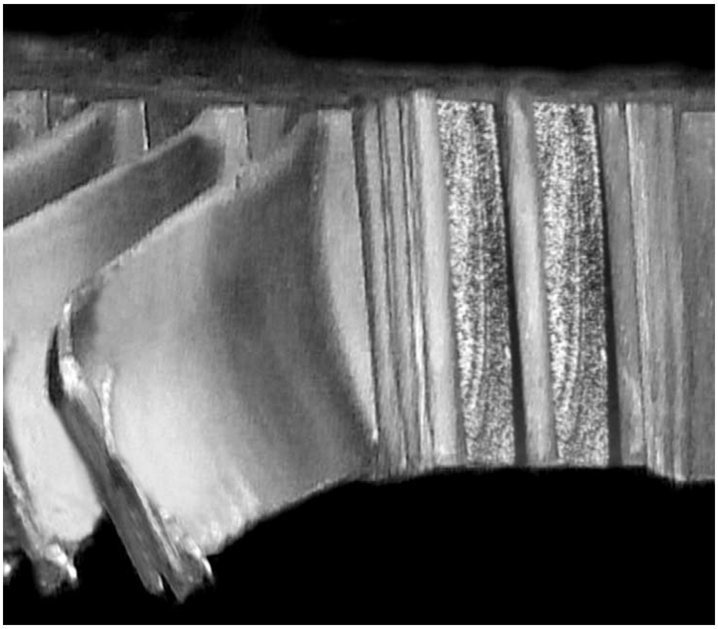

Fig. 2. View of the fractured disc.

Fig. 3 is a magnified view of the lower fracture surface. The curvature of the beach marks indicated that the incremental crack growth had taken place from the corner of the lug fracture region (zone A in Fig. 3). The fractured surface showed a clear difference in colour in two different regions. The crack origin zone, the fatigue fracture area with beach marks, and the ruptured zone are marked A, B and C, respectively. The region, which finally ruptured, is dark grey (C).

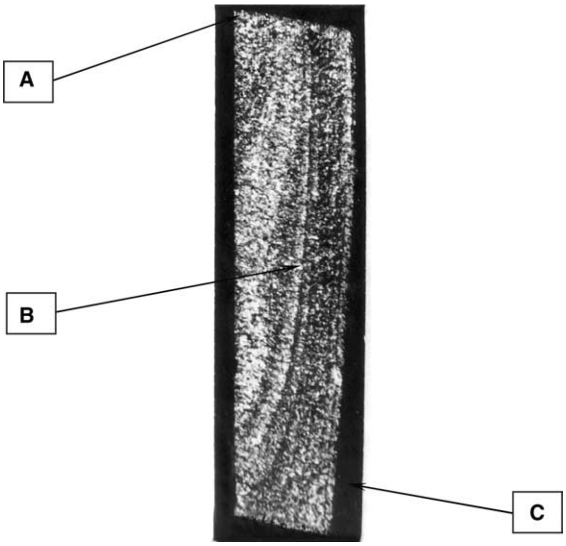

Fig. 3. Magnified view of the fractured surface.

3. Finite element model of the second stage turbine disc and the blade

Parametric geometry models of disc and blade were made, using the MSC-Patran 2004 program [10]. The FE model of disc presented in Fig. 4(a) consists of 11,220 nodes and 10,360 first-order, HEX-8 elements.

The discretized model of the blade, shown in Fig. 4(b) consists of 11,420 nodes, 13,248 first-order HEX-8 elements.

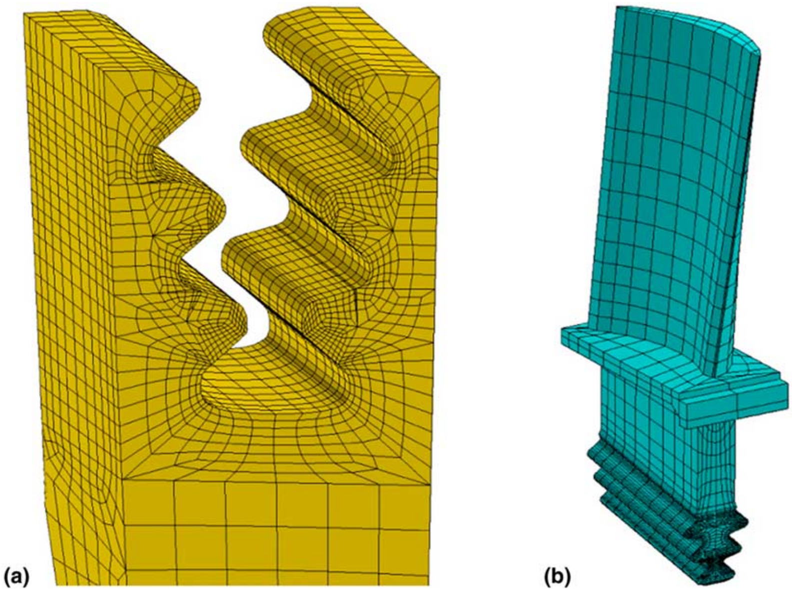

Fig. 4. Finite element models of the disc segment (a) and blade (b).

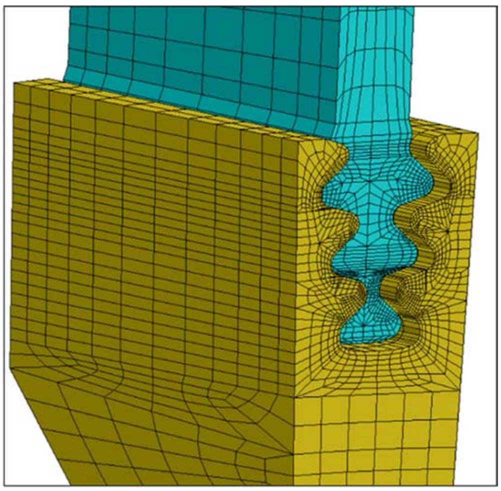

Fig. 5. Assembled model of the disc/blade segment in the vicinity of fir-tree slots.

To model the mechanical interface of adjacent surfaces of the disc and blade, the "master-slave" type of contact [10,11] with friction coefficient of 0.1 was defined.

The assembled model of the disc/blade segment is presented in Fig. 5.

4. Loads, boundary conditions and material properties for FE model

A rotating hot section component in a turbine engine is in general subjected to a combination of surface (aerodynamic) loads, centrifugal loads and thermal loads. The surface loads are associated with aerodynamic forces, resulting mainly from impingement of hot gases on the surfaces of blades. The centrifugal loads arising from the mass of the rotated disc and blades are usually the most critical loads acting on a turbine disc. This load was determined through finite element calculation after defining the axis of symmetry, the rotational speed and the disc and blade material density. In this analysis, the operational turbine speed of 12,500 rpm (rotation per minute) was applied. Computations for the rotational speed range of 0–25,000 rpm additionally were performed for analysis of phenomena occurring in the turbine during excessive speed.

The aerodynamic forces were modeled in the simplified procedure as two vectors of 100 N, imposed on the concave surface of blade. The simplified thermal load presented in Fig. 6 was defined.

The turbine disc is manufactured out of H-46 material. This alloy is a precipitation-hardened nickel-base superalloy with good strength, ductility, and fracture toughness over a temperature range of −50 to 600 °C. These properties along with good weldability and formability account for its wide use in aerospace applications. The yield point of H-46 alloy is 921 MPa, while the UTS (ultimate tensile strength) is 1200 MPa [12].

The blades for the turbine are manufactured out of E1-867 material. This alloy is a precipitation-hardened nickel base alloy, with better creep-resistance for high temperature. The analysis presented in this paper was performed for elastic–plastic disc and blade materials, with isotropic hardening.

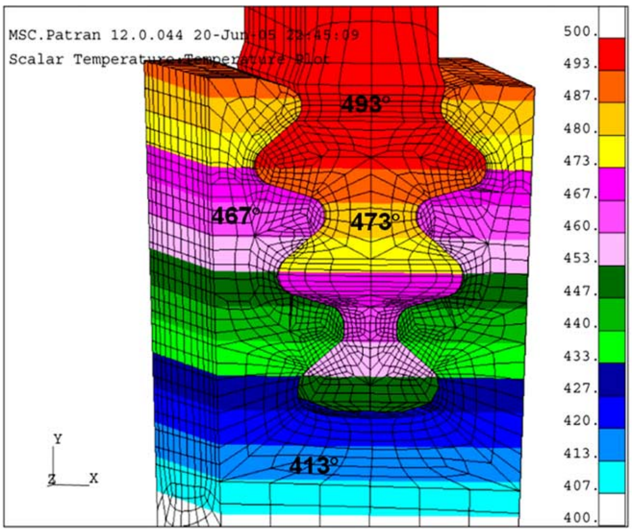

Fig. 6. Thermal field defined for models of disc and blade in the dovetail-rim region (Celsius scale).

5. Results of the finite element calculations

The ABAQUS v. 6.4 [11] program was used for stress analysis of the turbine disc. The nonlinear (incremental), Newton–Raphson method was applied. All computations were performed on 2-processor Sun Enterprice 3000 workstation in Computer Centre of the Rzeszow University of Technology. For all results, Megapascal (MPa) units were used to describe the fields of stress.

Fig. 7(a) shows that the area of the maximum Von Mises stress (968 MPa) for the operational speed of 12,500 rpm is located on the corner of the 3rd lower slot of the disc. The value of maximum principal stress for this critical zone is 1020 MPa (Fig. 7(b)). The second result (Fig. 7(b)) is particularly interesting from the point of view of the fatigue strength because just the tensile stresses contribute the most to the fatigue crack and then to crack propagation. The Von Mises stress distribution does not show if the material in tension or compressed. The location of the stress peak shown in Fig. 7 overlaps the fracture region presented in Fig. 2. The high level of stress in this area was the main reason for crack initiation in this region of disc. The fatigue loads (combination of the low cycle fatigue (LCF), thermal fatigue (TF) and high cycle fatigue (HCF)) caused the successive growth of the crack to critical size and then to rupture in the lower slot of the serrations.

A considerably lower value of stress (704 MPa) in the region of the fir-tree slots of blade can be observed in Fig. 8(a). The remaining zones of blade are not as highly loaded as the serration region. The maximum Von Mises stress in the middle region of the blade is only 400 MPa, whereas in the top the stresses have a range of 100–200 MPa (Fig. 8(b)).

The additional goal of this work was to indicate the critical areas with excessive rotational speed. For that purpose, in the numerical model the following characteristic points, presented in Fig. 9 were specified:

(1) Top part of the blade;
(2) Bottom part of the blade (connection between fir-tree slots and blade);
(3) Outside corner of the disc;
(4) Corner of 3rd lower slot of the dovetail-rim region of disc;
(5) Central part of disc;
(6) Bottom part of disc.

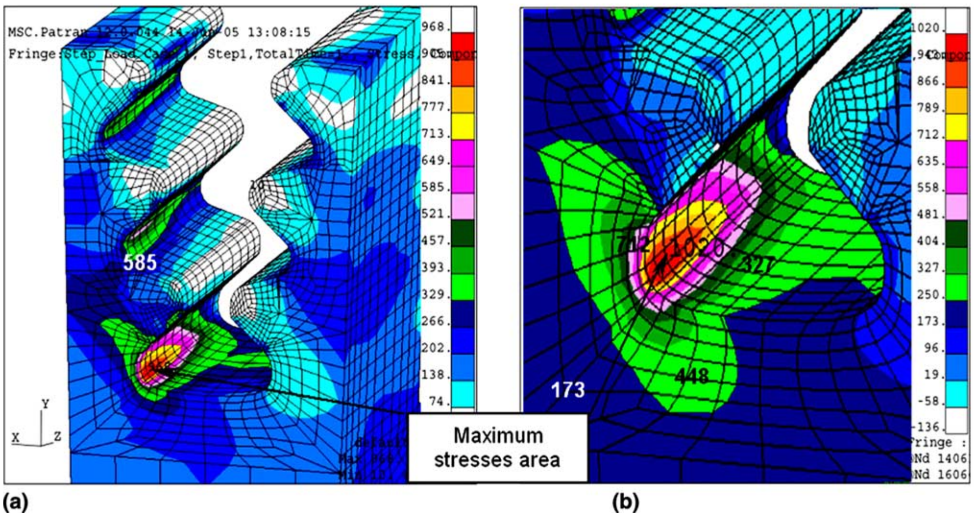

Fig. 7. Von Mises (a) and maximum principal (b) stress distribution in the vicinity of the serration area of disc for speed of 13,500 rpm.

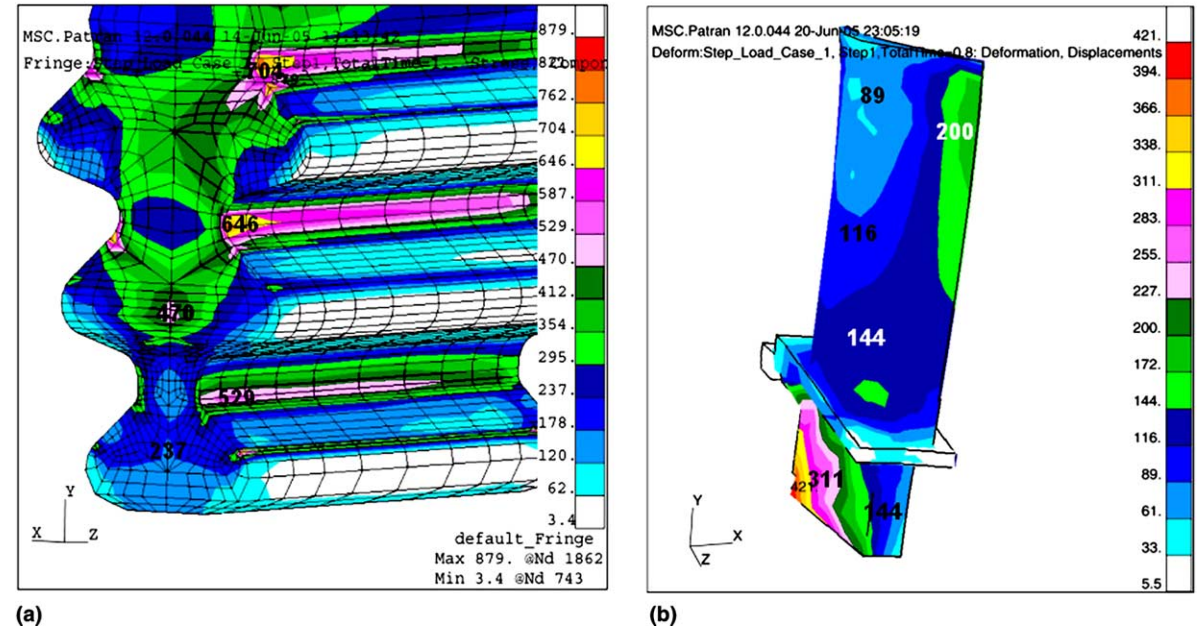

Fig. 8. Von Mises stress distribution in the fir-tree slots of blade (a) and for top part of blade (b), 13,500 rpm. The stresses are displayed on the deformed model with visualization scale of 25:1.

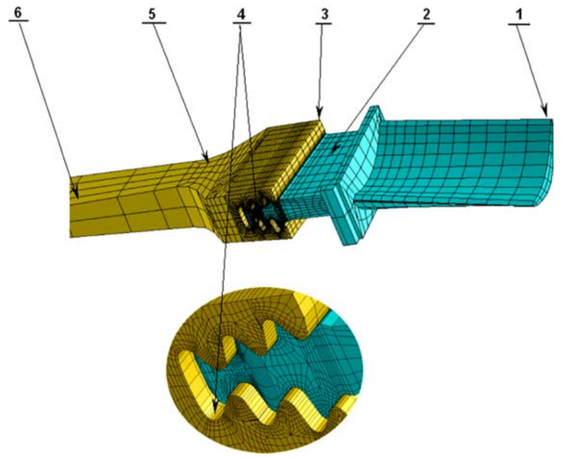

Fig. 9. Specified control points of turbine.

The specified points were useful to control the stresses and plastic strains of the turbine during its acceleration from 0 to 25,000 rpm.

According to the FEA simulation, Fig. 10(a) illustrates the values of Von Mises stresses for specified characteristic points of turbine for the speed range of 0–25,000 rpm. As seen from this figure, the curve nr 4, defined for critical region of disc has a maximum rate of stress increase for the speed range of 0–16,000 rpm (maximum, operational speed for considered turbine engine is 12,200 rpm). The clear change

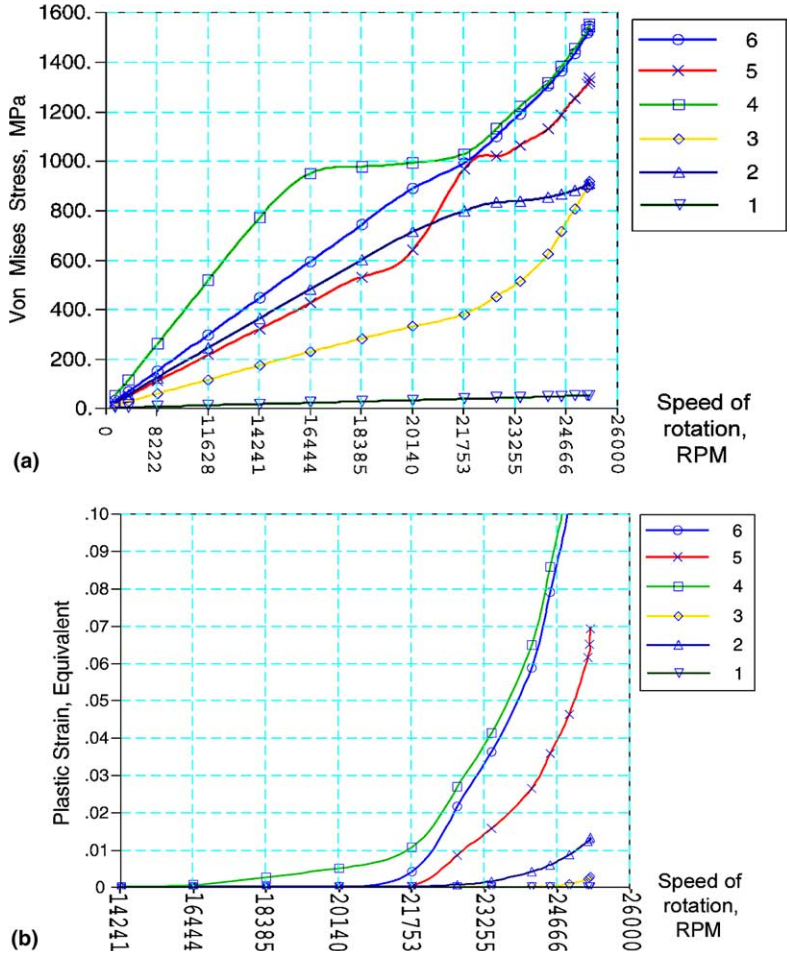

Fig. 10. Von Mises stress (a) and plastic strain magnitude (b) vs. rotational speed of turbine for selected control points.

of the line (nr 4) gradient at 16,000 rpm is related to the first plastic yield area in the lower fir-tree slot of the disc (see Fig. 10(b)).

The constant rate of plastic strain increase (Fig. 10(b)) is observed for the line nr 4 from 16,000 rpm until about 20,000 rpm. The next plastic strain area occurs at 20,000 rpm in the bottom part of the disc (point nr 6 in Fig. 10(b)). For 21,753 rpm, the plastic yield area enlarges and reaches the central part of the disc (point nr 5).

6. Conclusions

In this study the fracture analysis was performed to investigate the damage mechanisms of the turbine disc. To solve this problem, a geometrically complicated FE model with some nonlinearities as contact and elastic–plastic material was created. This study explains the reasons for catastrophic failure of the turbine disc. The analysis performed for several conditions has indicated a few critical regions of the turbine, with operational and excessive rotational speed. The first critical area is located on the corner of the 3rd lower slot of the dovetail-rim region of the disc, where the maximum stress was observed. Fracture of the disc in this zone can occur in the speed range of 14,500–16,000 rpm due to excessive stresses. Damage of the turbine wheel is possible also at lower speed, when the volume of the disc will contain a preliminary fatigue crack. However, accurate estimation of the maximum permissible speed as a function of crack size is possible only with a fracture mechanics analysis.

The second dangerous area of the disc is also its middle zone, which can yield at 20,000 rpm. Fracture of the turbine in this zone is very dangerous because the engine casing can be punctured by the larger fragments of the disc. However, the probability of this failure is very small because the speed of 20,000 rpm can only be obtained after disconnection of turbine and compressor.

7. Recommendations

(a) Increase the radius of the lower slot of the serration fitting.
(b) Change the dimensional tolerance of the dovetail-rim area of the turbine to unload the critical zone of the 3rd lower slot of the disc.

References

[1] Chan SK, Tuba IS. A finite element method for contact problems of solid bodies – Part II: Applications to turbine blade fastenings. Int J Mech Sci 1971;13:627–39.
[2] Masataka M. Root and groove contact analysis for steam turbine blades. Jpn Soc Mech Eng Int J 1992;35:508–14.
[3] Meguid SA, Kanth PS, Czekanski A. Finite element analysis of fir-tree region in turbine disc. Finite Element Anal Des 2000;35:305–17.
[4] Papanikos P, Meguid SA, Stjepanovic Z. Three-dimensional nonlinear finite element analysis of dovetail joints in aero-engine discs. Finite Element Anal Des 1998;29:173–86.
[5] Zboinski G. Physical and geometrical non-linearities in contact problems of elastic turbine blade attachments. J Mech Eng Sci 1995;209:273–86.
[6] McEvily A. Failures in inspection procedures: case studies. Eng Failure Anal 2004;11:167–76.
[7] Hou J, Wicks BJ, Antoniou RA. An investigations of fatigue failures of turbine blades in a gas turbine engine by mechanical analysis. Eng Failure Anal 2002;9:201–11.
[8] Bhaumik SK. Failure of turbine rotor blisk of an aircraft engine. Eng Failure Anal 2002;9:287–301.
[9] Park M, Hwang Y, Choi Y, Kim T. Analysis of a J69-T-25 engine turbine blade fracture. Eng Failure Anal 2002;9:593–601.
[10] MSC-PATRAN User's Manual, ver. 2004, MSC Corporation, Los Angeles; 2004.
[11] ABAQUS User's Manual, ver. 6.4, Abaqus Inc.; 2003.
[12] Astahow MF, Aircraft design – stability of structures, Moscow; 1954 [in Russian].